Vol. 21, No. 3(2022) Mat2832
Revista Mexicana de Ingeniería Química

Study of corrosion in metallic materials during the hydrodeoxygenation of palm oil in continuous fixed-bed reactor

Estudio de la corrosión en materiales metálicos durante la hidrodesoxigenación de aceite vegetal de palma en reactor de lecho fijo en flujo continuo

M. Cruz, G. Marroquín*, P. M. Vega-Merino, R. Guzmán, P. Rayo

Instituto Mexicano del Petróleo, Eje Central Lázaro Cárdenas Norte 152, San Bartolo Atepehuacan, 07730, México.

Received: May 23, 2022; Accepted: October 8, 2022

Abstract

In this work, corrosion damage in different metallic materials directly exposed to the corrosive environment generated in the catalytic hydrodeoxygenation (HDO) of palm oil to obtain green diesel in a continuous fixed-bed reactor at pilot plant scale was studied. Coupons were manufactured according to ASTM methods and were placed in holders at the outlet of the catalytic bed. Two experimental sets of 392 and 600 h of exposure time were carried out, keeping temperature and pressure at 340°C and 5 MPa, respectively, and results were reported as corrosion rate. It was found the material with the highest Cr content had the highest corrosion resistance. Similarly, it was noticed the most significant corrosion damage occurred just at the outlet of the catalytic bed. The experimental methodology followed in this work is a new procedure developed for continuous flow processes and could be used in transformation processes studies of biomass or other types of chemical compounds.

Keywords: corrosion rate, metallic materials, hydrodeoxygenation, palm oil, pilot plant.

Resumen

En este trabajo se estudió la corrosión de diferentes materiales metálicos, los cuales fueron expuestos directamente al ambiente corrosivo generado en la reacción de hidrodesoxigenación (HDO) catalítica del aceite vegetal de palma para la obtención de diésel verde, en flujo continuo a escala planta piloto. Los cupones fueron manufacturados de acuerdo con métodos ASTM y se colocaron en porta-cupones ubicados a la salida del lecho catalítico del reactor. Se realizaron dos pruebas experimentales a 392 y 600 h de tiempo de exposición, manteniendo constantes la temperatura en 340°C y presión de 5 MPa. El estudio se realizó en términos de la velocidad de corrosión encontrándose que el material con el mayor contenido de Cr presentó la mayor resistencia al deterioro. Asimismo, se encontró que el mayor daño por corrosión ocurrió justo a la salida del lecho catalítico del reactor. La metodología experimental aplicada y desarrollada en este trabajo es un procedimiento nuevo que podría utilizarse en el estudio de otros procesos en flujo continuo de transformación de biomasa u otros tipos de compuestos químicos.

Palabras clave: velocidad de corrosión, material metálico, hidrodesoxigenación, aceite de palma, planta piloto.

* *Corresponding author. E-mail*: gmarroq@imp.mx
https://doi.org/10.24275/rmiq/Mat2832
ISSN:1665-2738, *issn-e*: 2395-8472

1 Introduction

One of the most frequent concerns in different industry branches is the corrosion problem, which refers to the destruction or degradation of metallic material by reaction with its environment, where the metal is transformed either into oxide or any other compound, deteriorating their original physical and chemical properties. Corrosion is a gradual chemical or electrochemical attack that affects carbon steels, that is, low-alloy steels that are susceptible to corrosion attacks due to the interaction with different prevailing environments or simply because it tends to react with oxygen in the medium.

Different factors influence the corrosion process, such as solution acidity, dissolved salts, substances nature, protective layers, oxygen concentration, temperature, flow rate, and exposure time (Salazar-Jiménez, 2015). Therefore, the form and corrosion rate vary depending on the metal type, and corrosive environment.

Corrosion phenomenon jeopardizes production systems and useful life of commercial facilities and human lives due to collapse risk. Corrosion occurs in all industries, e.g., hydrocarbons extraction, transportation, refining, and other chemical transformation processes (Askari *et al*., 2019; Groysman, 2017; Mansoori *et al*., 2017).

A recent industry that has been growing up is the transformation of biomass into biofuels, mainly vegetable oils or animal fats into biodiesel and green diesel, which can be obtained through transesterification and hydrodeoxygenation (HDO), respectively. Biomass is mainly constituted by triglyceride with an ester group, with carbon chain length ranging from C_8 to C_{24} (Mailaram *et al*., 2021; Sotelo-Boyas *et al*., 2012), that is, the same carbon range of the fossil diesel. Consequently, transesterification converts triglycerides (ester) to another ester (FAME: Fatty Acid Methyl Esters or biodiesel), using light alcohol, NaOH or KOH as a catalyst, obtaining glycerin as by-product (Kant Bhatia *et al*., 2021; Tabatabaei *et al*., 2019). Transesterification is a simple process that does not require economies of scale and it is operated at atmospheric pressure and temperatures between 50 and 80°C (Ambat *et al*., 2018; Chozhavendhan *et al*., 2020; Tabatabaei *et al*., 2019).

On the other hand, HDO is a pathway for triglyceride conversion to obtain green diesel consisting mainly of paraffin mixtures (Bezergianni and Dimitriadis, 2013). To promote the HDO reactions, high pressure and temperature, and NiMo/γ-Al_2O_3 or CoMo/γ-Al_2O_3 catalysts are required (Cavani *et al*., 2016; Douvartzides *et al*., 2019; Perego and Ricci, 2012). A mixture of H_2O, CO_2, and CO obtained as by-product may cause corrosion damage to process lines, reactor, and other equipment under high temperature and pressure.

In open-access literature, there is a lack of information about the corrosion effect during the green diesel production; however, some research studies of corrosion caused by biofuel by-products are reported and briefly described as following:

Da Mota *et al*. (da Mota *et al*., 2014) studied the green diesel production by thermal catalytic cracking of palm oil, using a carbon stainless steel reactor (ASTM 409) of 143 L operating in batch mode at 450°C and atmospheric pressure. Products were characterized by a copper corrosion test, observing that low content of oxygenated compounds gives low corrosive characteristic and excellent thermo-oxidative stability to the green diesel.

Cabrini *et al*. (2017) performed a study about the corrosive behavior of austenitic stainless steels AISI 316L and AISI 304L during the liquefaction process of a simulated organic fraction of municipal solid waste. The liquefaction reaction was carried out in a batch reactor with temperatures ranging 240-250°C and at 300°C, from 55 up to 264 h of exposure time, and pressure between 3.9 and 9.8 MPa. Results showed meager corrosion rates strictly dependent on the exposure time and temperature. Pitting corrosion initiation was only observed in AISI 304L steel.

Keiser *et al*. (2012) studied corrosion of coupons of different materials using bio-oil obtained by pyrolysis of biomass. Bio-oil was fed to a batch reactor with immersed coupons and U-bend stress corrosion cracking coupons of various materials, such as carbon steel, 2 ¼ Cr-1Mo steel, and 409, 304L, and 316L stainless steels. Corrosion tests were carried out at a maximum temperature of 50°C and exposure times of 250, 500, and 1000 h. The authors found that there was a localized crack-like attack, in some cases related to grain boundaries. Also, accelerated stress corrosion occurred in the low alloy steels. Although only few samples were cracked, these results concerned the potential for stress corrosion cracking.

As it can be noticed, experiments for corrosion studies reported in open-access literature were carried out with products obtained from biomass conversion in batch reactors. That is, there is a lack of experimental

studies about the corrosive effect at the conditions of biomass conversion as well as by-products obtained. This work reports the corrosive effect on different coupons of metallic materials caused by the corrosive environment derived from the conversion of palm oil to green diesel, H_2O, CO_2, and CO, at pilot plant, in a continuous fixed-bed reactor, at given operating conditions.

2 Experimental methodology

2.1 *Pilot plant description*

Palm oil HDO tests were carried out in a pilot plant in which 100 mL of commercial NiMo / γ-Al_2O_3 catalyst was placed in a fixed-bed reactor continuously operated. Figure 1 shows the pilot plant configuration used in the experiments. The pilot plant has the following main sections: feed section, reaction section, separation section, online measurement, and analysis system for reaction gases. The reactor operates isothermally with downstream flow; it has an internal diameter of 25.4 mm and a length of 1430 mm. The catalyst loading, presulfiding and start-up procedures were described in detail in a previous study (Marroquín-Sánchez and Ancheyta-Juárez, 2001). The pilot plant is often used for hydrodesulfurization of middle distillates, and in this case, for the HDO of palm oil.

2.2 *Experimental conditions*

Palm oil hydrodeoxygenation was carried out at constant conditions: temperature of 340°C, pressure of 5 MPa, feed flow of 100 mL/h, and H_2 flow of std 135 L/h (0°C, 1 atm). The temperature, pressure, and feed and H_2 flows were the same for the two experimental sets but the exposure times were 392 and 600 h for sets 1 and 2, respectively. The operating conditions were selected based on reported data in previous works as references (Cavani *et al*., 2016; Verduzco *et al*., 2020). Hydrogen with 99.9% purity was used.

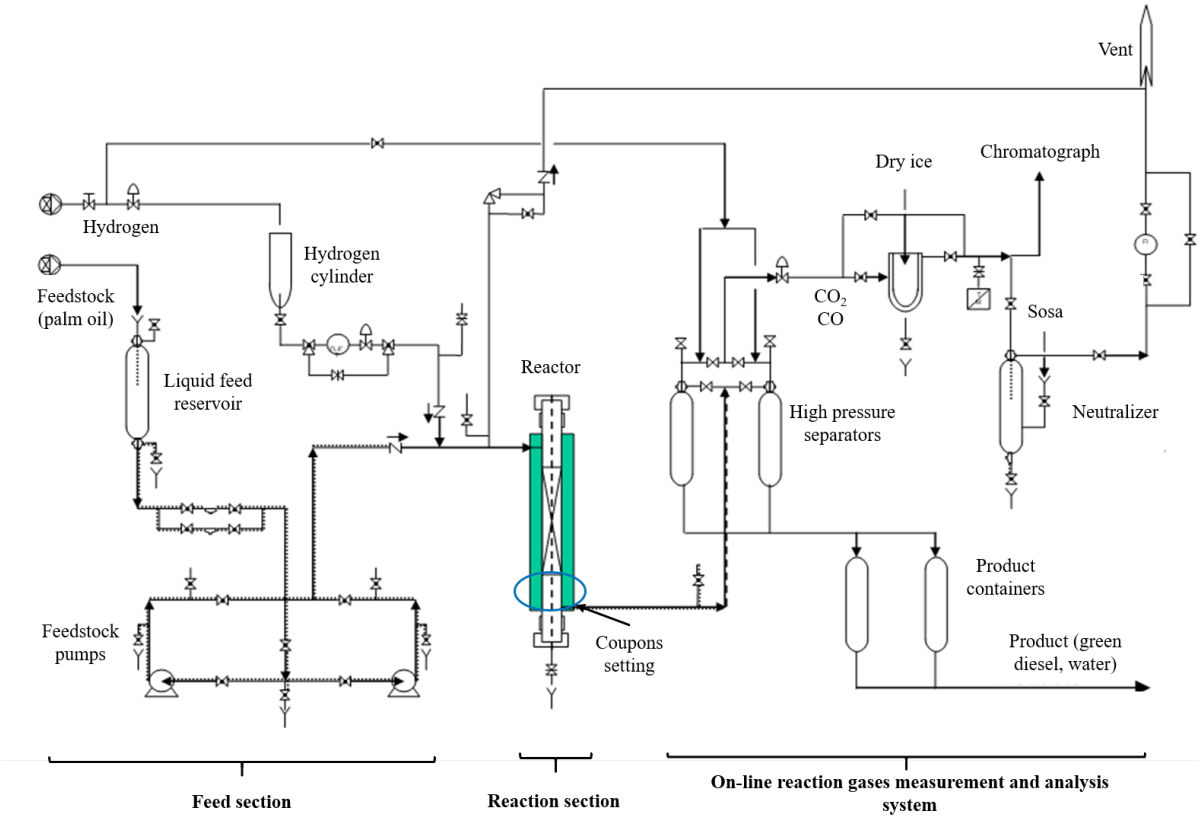

Figure 1. Pilot plant scheme to produce green diesel by HDO of palm oil.

Table 1. Chemical composition of metallic materials used in the manufacture of coupons.

Material	C, Max	Mn, Max	P, Max	S, Max	Si, Max	Ni, Min	Cr, Min	Mo, Min	N, Min	Cu
TP410	0.15	1	0.04	0.03	1		11.5-13.5			
A179	0.06-0.18	0.27-0.63	0.035	0.035	0.25					
1010	0.08-0.13	0.25-0.4	0.04	0.05						
304	0.08	2	0.045	0.03	0.75	8.0 - 10.5	18-20			
316	0.08	2	0.045	0.03	0.75	10.0 - 14.0	16.0 - 18.0	2.0- 3.0	0.1	
316L	0.03	2	0.045	0.03	0.75	10.0 - 14.0	16.0 - 18.0	2.0- 3.0	0.1	
347	0.08	2	0.045	0.03	0.75	9.0- 13.0	17.0 -19.0			
P11	0.05-0.15	0.3-0.6	0.025	0.025	0.5-1.0		1.0-1.5	0.44-0.65		
P9	0.15	0.3-0.6	0.025	0.025	0.25-1.0		8.0-10.0	0.9-1.1		
Cr0.65		0.93		0.224	1.03		0.641	0.022		
Cu										100

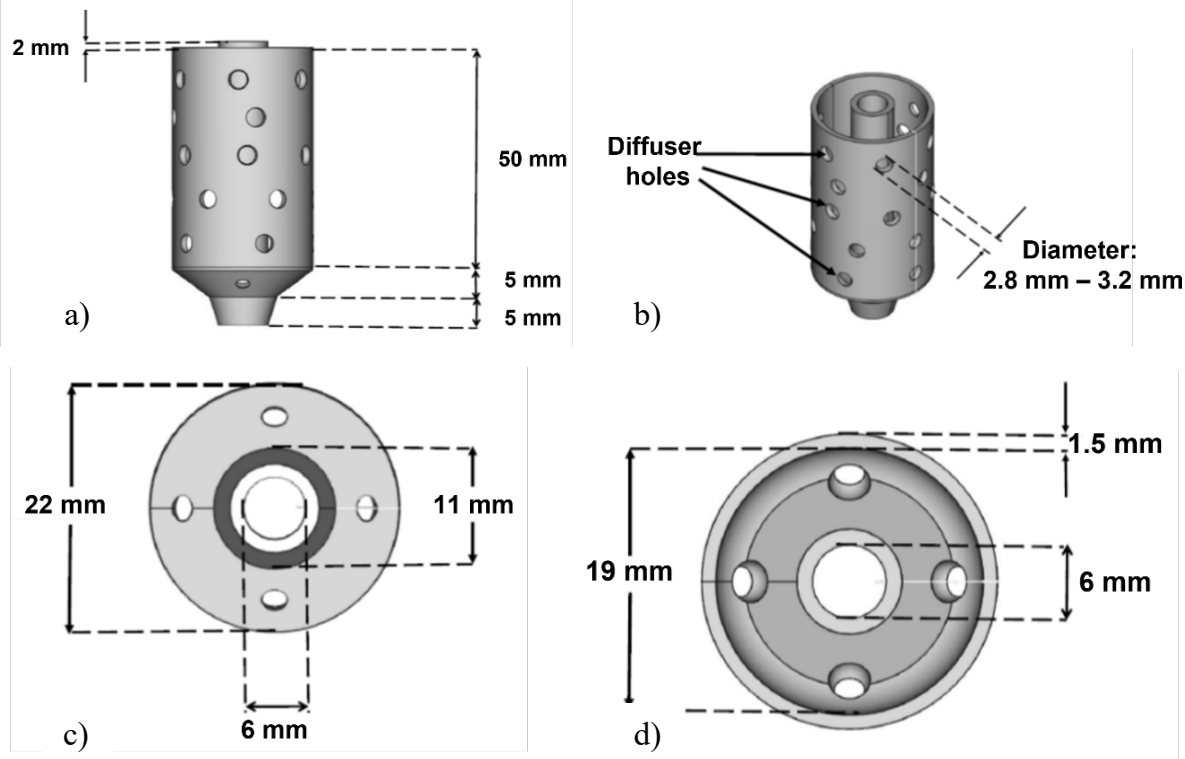

Figure 2. Coupon holder dimensions: a) Side view, b) Axial view, c) Bottom view, d) Top view.

2.3 Metallic materials

Table 1 shows the chemical composition of metallic materials used in the two experimental tests. The metallic materials were TP410, A179, 1010, 304, 316, 316L, 347, P11, P9, Cr0.65, and Cu. The materials were selected based on their ability to withstand high temperature and pressures in chemical transformation processes, except Cu.

2.4 *Coupon holder design*

The coupon holder was designed considering the following aspects:

1. Reactor diameter and length
2. Avoid contact between coupon and reactor surface to prevent galvanic corrosion
3. High-temperature resistant materials

Figure 2 shows coupon holder dimensions. Figure 2a shows coupon holder length, whose outer tube has a size of 50 mm at the bottom, it has 10 mm with a diameter reduction to join with the inner tube; this inner tube is used to set the thermowell for measuring process temperature and it is also used to join another coupon holder. The outer tube was perforated with holes from 2.8 to 3.2 mm (Figure 2b) that allow reaction products circulation in a liquid and gaseous phase, and Figures 2c and 2d show a bottom and top view of the coupon holder, respectively. The outer tube has an external diameter of 22 mm and an internal diameter of 19 mm, while the inner tube has an external diameter of 8 mm, and an internal diameter of 6 mm. Coupons were placed into the separation between tubes.

2.5 *Coupon dimensions*

Specimens shape and dimensions vary with the test purpose and test apparatus (NACE TM0169/ASTM G31, 2021). Corrosion coupons dimensions must allow their exposed areas calculation in a simple and precise way (NACE TM0169/ASTM G31, 2021).

Based on pilot plant reactor dimensions used in this work, Figure 3 shows two corrosion coupon types with the following dimensions:

- Type I coupon. 16 mm height, 12 mm width, and 1.5 mm thickness (Figure 3a).
- Type II coupon. 32 mm height, 13 mm width, 1.5 mm thickness (Figure 3b).

2.6 *Corrosion coupon preparation*

Coupons were made with the materials shown in Table 1, using the dimensions of Figure 3; polishing the edges and the surface with abrasive paper. Subsequently, these were treated based on the following procedure:

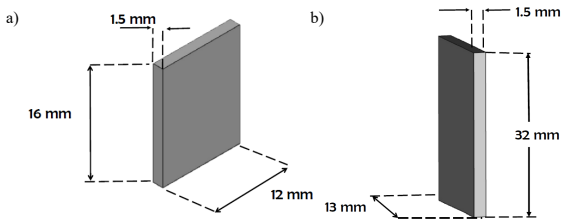

Figure 3. Coupons dimensions. a) Type I coupon, b) Type II coupon.

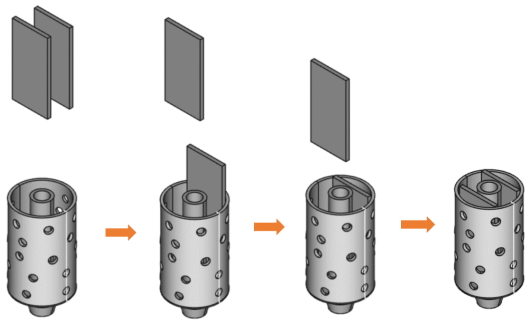

Figure 4. Setting sequence of coupons in the coupon holder.

- Coupons were labeled for easy identification.
- Coupons were cleaned with isopropyl alcohol, subsequently with acetone; then, coupons were dried at room temperature.
- Exposed surface area of each coupon was calculated.
- Coupons were weighted on an analytical balance with a sensitivity of ± 0.1 mg.
- Coupons were wrapped in anticorrosive paper, silica gel, and placed into a desiccator for their conservation.

2.7 *Coupons setting in the coupon holder*

Figure 4 shows the sequence of coupons placement inside the coupon holder. Two coupons can be placed vertically in each coupon holder, either the same material or different metallic materials. The space between the coupons and the coupon holder was filled with borosilicate spheres around 3 mm of diameter.

Table 2. Metal coupons setting.

Coupon holder number	Set 1	Set 2
I	304-A	P11-A
	304-B	Cu-A
II	316L-A	Cr0.65-A
	316L-B	P9-A
III	TP347-A	P11-B
	TP347-B	Cr0.65-B
IV	316	Cr0.65-C
	SAE 1010	P9-B
V	A179	P11-C
	TP410	Cu-B

2.8 *Loading coupon holders inside the pilot plant reactor*

Coupon holders loading inside the reactor was carried out as the following: coupon holders were inserted with the coupons and placed in series at reactor bottom. Subsequently, the thermowell was placed inside the inner tube of each coupon holder. The loading started with a bed of glass wool, then a bed of NiMo/γ-Al_2O_3 catalyst, after a bed of glass wool, and finally, at the reactor top, a bed of alumina spheres approximately 3 mm in diameter (inert material). It was possible to use 5 coupon holders simultaneously for the same experimentation inside the reactor. Three thermocouples were placed inside the thermowell to measure the temperature in the preheating zone (zone 1), reaction zone (zone 2), and the outlet of the catalytic bed of the reactor (zone 3).

2.9 *Experimental sets*

Two experiments sets were established for corrosion assessment on metallic materials exposed to palm oil HDO process:

Set 1. Metallic materials 304, 316L, TP347, 316, SAE 1010, A179, and TP 410 were exposed. Coupon holders were identified as I, II, III, IV, and V, in which the coupons shown in Table 2 were located.

Set 2. Metallic materials identified as P11, P9, Cr0.65, and Cu were exposed; their location is shown in Table 2.

The coupon holder I was located at the catalytic bed outlet, and later coupon holders II, III, IV, and V. The coupon holder V was placed at the reactor outlet. The aim of studying the experimental set 1 with the metallic materials in coupon holders I, II, and III was to determine the corrosion rate behavior with the same material type, while with the experimental set 2, the position effect of metallic material in the reactor was studied.

2.10 *Reactor hermeticity test, catalyst activation, reaction test, pilot plant shutdown, and coupon unloading*

After the catalyst and coupon holders were installed, the reactor was hermetically sealed. Next, a hermeticity test was carried out with nitrogen at room temperature and a pressure of 7 MPa for 2 h. Subsequently, the catalyst was activated following the methodology reported in a previous study (Marroquín *et al*., 2004). At the catalyst activation ending, straight run gas oil and hydrogen were fed, and the pressure was set at 5 MPa. Simultaneously, the temperature was increased from 315 to 340°C at a rate of 10°C/h. Under these conditions, a stabilization period was carried out for 70 h. Subsequently, the reactor was fed with palm oil and hydrogen, maintaining the pressure and temperature at 5 MPa and 340°C, respectively, and the system was stabilized for 20 h. After this stabilization, palm oil hydrodeoxygenation experimentation was started to study the corrosive effect of reaction by-products (H_2O, CO_2, CO, unreacted H_2) on metal alloys. For each set of experiments mentioned in 2.9, a load of new catalyst was used.

According to the literature, the exposure times for corrosion studies using bio-oils vary between 264 and 1000 h (Cabrini *et al*., 2017; da Mota *et al*., 2014). Based on the foregoing, the duration of the experimental sets 1 and 2 were 392 and 600 h, respectively (these are also the exposure times of the metallic materials with the corrosive environment). In addition, the exposure time of experimental set 1 was established because this time allows to observe the damage in metallic materials at the laboratory level. The exposure time of experimental set 2 is the time frequently used in a semi-industrial plant for demonstration test, thus, this exposure time was fixed to evaluate corrosion damage in metallic material. Both experiments were carried out in continuous flows.

The pilot plant shutdown considered a methodology described in previous works (Marroquín *et al*., 2004). Having the pilot plant at room temperature and atmospheric pressure, the reactor was opened. Coupon holders with the metallic coupons were uninstalled as shown in Figure 5. Subsequently, the spent catalyst was unloaded.

Table 3. Constants for the corrosion rate for equation 1 (ASTM G1, 2017; ASTM G31, 2021).

Corrosion Rate Units	Constant (K) in Corrosion Rate Equation
Mils per year (mpy)	3.45×10^{6}
Inches per year (ipy)	3.45×10^{3}
Inches per month (ipm)	2.87×10^{2}
Millimetres per year (mm/y)	8.76×10^{4}
Micrometres per year (μm/y)	8.76×10^{7}
Picometres per second (pm/s)	2.78×10^{6}

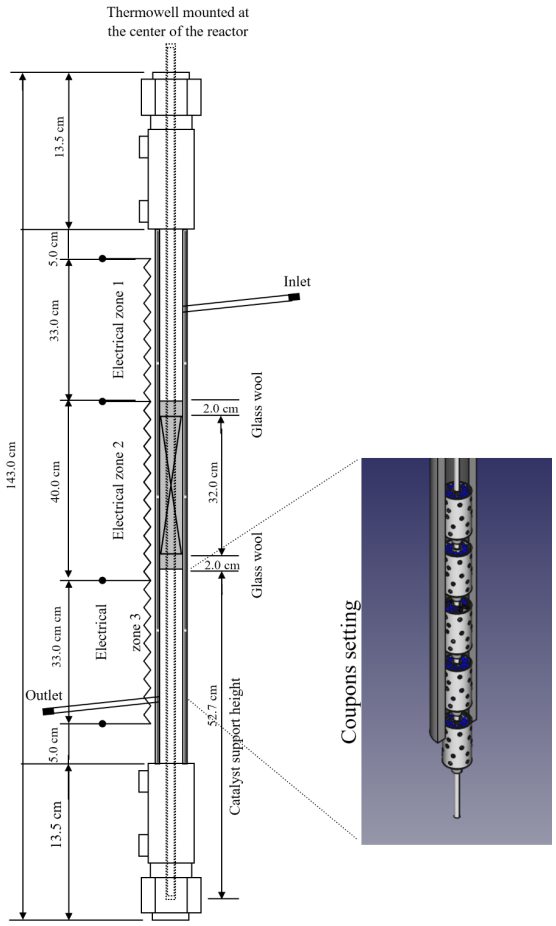

Figure 5. Coupon holders setting inside the reactor.

2.11 *Treatment and weighting of evaluated coupons*

Each coupon exposed to the corrosive environment of HDO reaction was cleaned with isopropyl alcohol and acetone to remove any deposited residue, dried, and weighted with an analytical balance with a sensitivity of ±0.1 mg.

Table 4. Corrosion rate levels per year (NACE RP0775, 2018).

Corrosion level	Uniform corrosion rate	
	mm/y	mpy
Low	<0.025	<1.0
Moderate	0.025-0.12	1.0-4.9
High	0.13-0.25	5.0-10.0
Severe	>0.25	>10.0

2.12 *Corrosion rate estimation*

The mass loss suffered of the metallic material was calculated by the difference between the initial and final mass of each coupon, assuming that the corrosion was uniform; therefore, the corrosion rate was estimated only by the gravimetric method. According to the ASTM G1 and ASTM G31 methods, the corrosion rate was calculated by applying the following equation (ASTM G1, 2017; ASTM G31, 2021).

$$\text{Corrosion rate} = \frac{K \times W}{A \times T \times D} \tag{1}$$

Where:

K = Constant, whose value depends on the units in which corrosion rate is expressed (Table 3)

W = Mass loss, g

A = Area, cm^2

T = Exposure time, h

D = Density, g/cm^3

Corrosion rate values can be interpreted based on different deterioration degrees (Table 4), which are low, moderate, high, and severe.

Table 5. Composition of products obtained from the HDO of palm oil in a pilot plant.

Component	% weight
H_2	6.32
C_5=/C_6+	0.03
C_3H_8	3.68
C_3H_6	0.02
H_2S	0.07
i-C_4H_{10}	0.01
C_3H_4	0.01
CO_2	3.51
C_2H_6	0.07
CH_4	0.37
CO	1.09
Green diesel	78.14
H_2O	6.66

3 Results and discussion

3.1 *Corrosive environment*

At the reactor outlet, gas and liquid mixture was obtained. Reaction products composition is included in Table 5. The gas composition was determined by online chromatographic analysis. Unreacted hydrogen is the component with the highest concentration, followed by reaction gases, such as CO, CO_2, C_3H_8, CH_4, H_2S, and other light hydrocarbons of 1 to 6 carbon atoms. On the other hand, the liquid phase is a mixture of green diesel and H_2O. H_2O, CO_2, and CO is a corrosive mixture at high temperatures.

There is no information reported in the literature about the corrosion caused for free fatty acids contained in vegetable oils. It can be mentioned that the palm oil used in the experimental test has a low content of free fatty acids because the feedstock was refined previously; the experimental result of Total Acid Number was <0.18 mg KOH/g by method ASTM (ASTM D664, 2018), which is considered low value to cause corrosion damage in the HDO process, beside the free fatty acids are converted during palm oil transformation into green diesel; therefore, only H_2O, CO_2 and CO were considered as corrosive species.

3.2 *Experimental set 1*

Figure 6 shows the initial and final physical appearance of the coupons used in the corrosion test in the HDO process at 340°C for 392 h. It is observed that the coupons present a darkening on their exposed surface to the corrosive environment.

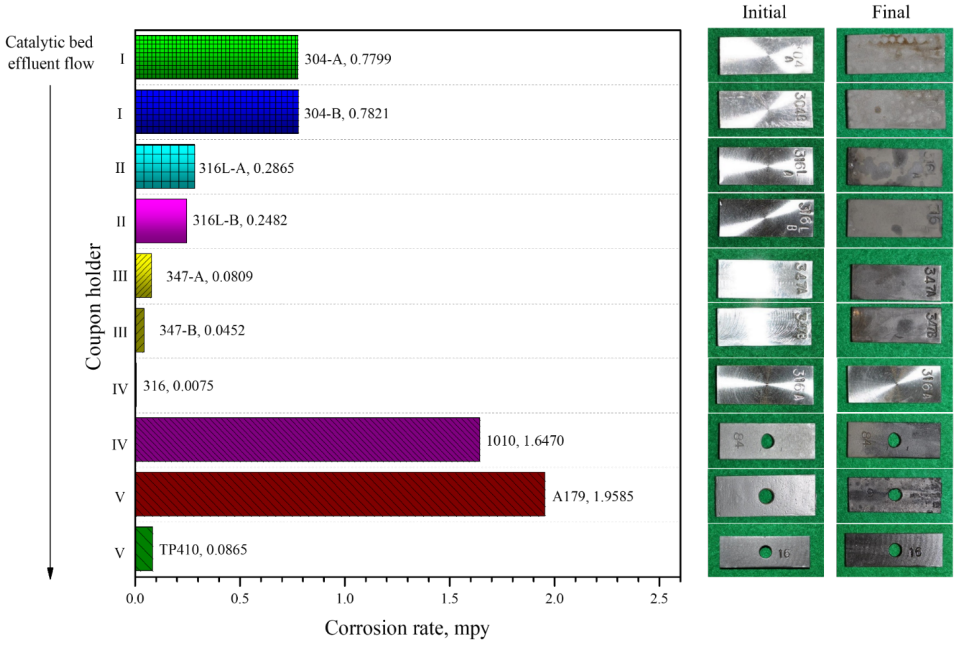

Figure 6. Corrosion rate, initial and final physical appearance of the metallic materials exposed to corrosive environment at 340°C for 392 h.

The corrosion rate was determined with the initial and final mass of each coupon, density, area, exposure time, and equation 1 (ASTM G1, 2017; ASTM G31, 2021). The results are shown in Figure 6. Coupon holders I, II, and III contained duplicated coupons of metallic materials. It was observed that the corrosion rate of each coupon of these coupon holders was very similar, which indicates that corrosion is uniform in the reactor transversal section. On the other hand, coupons made of different materials were set in coupon holders IV and V.

The lowest corrosion rate was presented by the coupon 316 located in the coupon holder IV, while the A179 coupon located in the V coupon holder presented a corrosion rate 261 times greater than that presented by coupon 316, being this material clearly susceptible to damage by contact with corrosive environment. In Figure 6, it is also observed that the corrosion rates in experimental set 1 presented an average of 0.6484 mpy and varied from 0.0075 to 1.9585 mpy. Thus, the corrosion rate in the experimental set 1 presented a high dispersion in their values, which means that there were materials with severe damage such as 1010 in coupon holder IV and A179 in coupon holder V, and other ones that were more resistant such as 316 in coupon holder IV and 347-B in coupon holder III.

Simultaneously, in Figure 6, the corrosion rate results of each exposed coupon were plotted, and based on the classification established in Table 4, the following corrosion levels were found:

- Coupons made with metals 304, 316L, 347, 316, and TP410 showed low corrosion levels (<1.0 mpy)
- Coupons 1010 and A179 had moderate corrosion levels (1.0-4.9 mpy).

Based on the characteristics included in Table 1, the materials identified as 316 and 347-B, which presented the lowest corrosion rates, contain Ni and Cr. In contrast, the materials identified as A179 and 1010, which showed the highest corrosion rates, lack these elements.

Most of the materials presented corrosion rates lower than 1.0 mpy, which refers to a low level of corrosion (NACE RP0775, 2018), therefore, these materials could be used in the HDO process of palm oil, guaranteeing the physical integrity of equipment and process lines.

In brief, all the steels evaluated showed good resistance to the corrosive environment generated by the products of the HDO reaction of palm oil to green diesel production. 304, 316L, 347, 316, and TP410 steels could be suitable for the palm oil HDO process.

Temperature measurements were made in the catalytic bed, and variations of 1 to 5°C were observed, which are considered acceptable variations for the pilot plant control system for the isothermal regime, hence, it is assumed that the system was maintained isothermally in the longitudinal reactor section and at the catalytic bed outlet the temperature was 340°C.

In this work, measuring the corrosion rate at different times was impossible since the reaction system configuration did not allow the exposed coupon recovery; it was only possible to determine the corrosion rate at the test ending. However, the corrosion rate is not expected to be linear as a function of time since at the beginning of the experimentation the metal surface is new, which allows more significant interaction with the corrosive medium. However, over time, the metal-corrosive medium interaction can decrease considerably when a corrosion products layer (oxides) forms. A corrosion rate study at different times was carried out by Farelas *et al* (2010) where at the beginning the rate increases reaching a maximum value and later, the corrosion rate remains constant.

3.3 Experimental set 2

In experimental set 2, four different materials were evaluated during the HDO of palm oil to obtain green diesel at 340°C for 600 h. Unlike experimental set 1, in this case, the coupons position was varied, and the exposure time was increased.

Figure 7 shows the initial and final physical appearance of each coupon. A color change of the exposed coupons is observed. The coupon Cu-A placed in the coupon holder I was disintegrated, only material remnants were found during the holder and catalyst unloading; therefore, the corrosion rate of this metal was not calculated. Consequently, Cu materials should not be used in equipment and lines for this process.

The corrosion rate was determined using the same procedure as experimental set 1, the results are shown in Figure 7. The lowest corrosion rate corresponds to the coupon P9-B located in coupon holder IV, while the higher corrosion rate corresponds to the coupon P11-A located in coupon holder I, which is 327 times greater than that calculated for coupon P9-B. It is also observed that the corrosion rates had an average of 3.4682 mpy, which varied from 0.0470 to 15.3896 mpy.

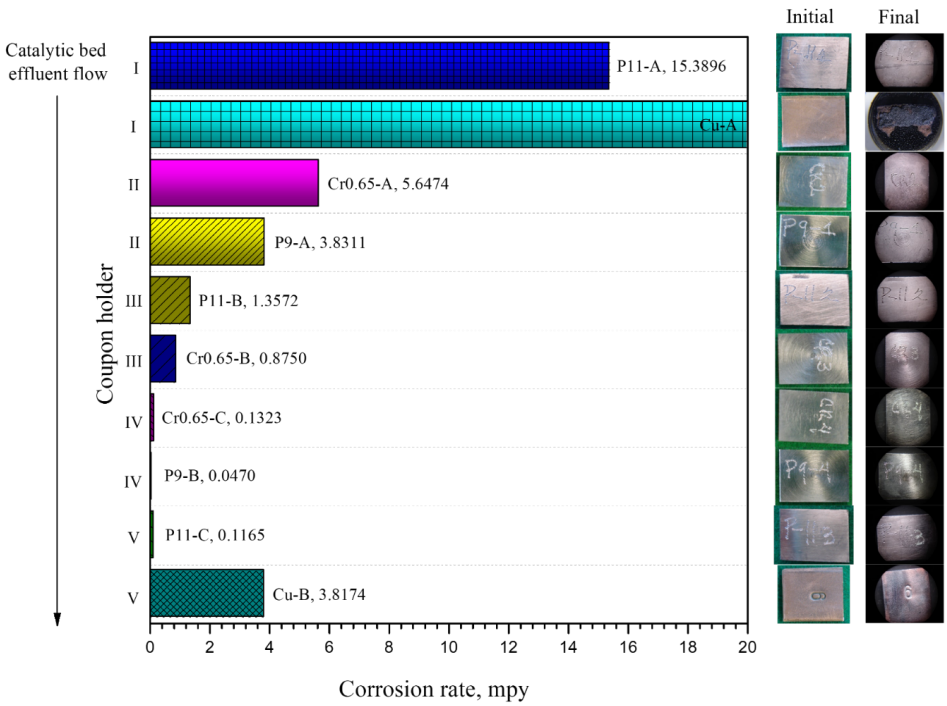

Figure 7. Corrosion rate, initial and final physical appearance of the metallic materials exposed to corrosive environment at 340°C for 600 h.

Hence, the corrosion rate of the materials considered in experimental set 2 presented high dispersion in their values, even higher than in experimental set 1 (Figure 6).

The average corrosion rate of experimental set 2 is greater than 1.0 mpy, a value that is not exceeded by the average corrosion rate of experimental set 1 (3.4682 vs 0.6484 mpy). Therefore, in experimental set 2 were found more severe damage such as P11 A and Cu A in coupon holder I.

The results of the corrosion rate of each exposed coupon were also plotted, according to the Figure 7, the corrosion rate depends on the position in which the coupons are placed in the reactor. Coupons made from the same material would be expected to exhibit similar corrosion rates; however, they are considerably different. This can be observed in coupon P11: coupon P11-A located at the catalytic bed outlet (coupon holder I) presented a severe corrosion rate of 15.3896 mpy, while coupon P11-B set in coupon holder III presented a moderate corrosion level of 1.3572 mpy, and coupon P11-C located in the coupon holder V showed a low corrosion level of 0.1165 mpy. The same downward trend was observed with the other three test metals; hence, corrosion was higher at the reactor outlet in all the materials considered in experimental set 2.

Based on the classification established in Table 4, the following corrosion levels are found:

- Coupons P11-A and Cu-A presented a severe corrosion level (> 10.0 mpy)
- Coupon Cr0.65-A exhibited a high corrosion level (5.0-10.0 mpy)
- Coupons P9-A, P11-B, and Cu-B showed a moderate corrosion level (1.0-4.9 mpy)
- Coupons Cr0.65-B, Cr0.65-C, P9-B, and P11-C presented a low corrosion level (<1.0 mpy).

According to the characteristics included in Table 1, the materials identified as P11, P9, and Cr0.65 lack Ni and have different Cr content, consequently, they have different corrosion rates.

The materials evaluated in experimental set 2 were less resistant than the materials used in experimental set 1 by contact with the corrosive environment. The different compositions of the test metals and the position at the outlet of the catalytic bed could have generated the observed differences.

The Cr content plays an important role in the materials corrosion resistance because Cr is

responsible for the passivation process by forming a thin protective layer of chromium oxide on the metal surface when Cr reacts with oxygen.

Conclusions

Hydrodeoxygenation of palm oil to green diesel generate a mixture of H_2O, CO_2, and CO, which is a corrosive environment at high temperature for various metallic materials.

The metallic materials evaluated in the experiments presented different corrosion rates, finding that the higher the Cr concentration, the lower the corrosion rate.

The corrosion rates of coupons with the same metallic material, placed in different positions but exposed to HDO reaction products were different. The most significant damage was just at the outlet of the catalytic bed.

The experimental methodology developed and followed for the corrosion damage assessment of metallic materials in the hydrodeoxygenation of palm oil at pilot plant scale in continuous flow can also be used for other chemical transformation processes of different types of biomass or other chemical compounds.

Acknowledgments

Authors thank Instituto Mexicano del Petróleo for supporting this research project. M.C. also thanks Consejo Nacional de Ciencia y Tecnología (CONACYT) for the Ph.D. Scholarship grant.

References

Ambat, I., Srivastava, V., and Sillanpää, M. (2018). Recent advancement in biodiesel production methodologies using various feedstock: A review. *Renewable and Sustainable Energy Reviews 90*, 356-369. https://doi.org/10.1016/j.rser.2018.03.069

Askari, M., Aliofkhazraei, M., and Afroukhteh, S. (2019). A comprehensive review on internal corrosion and cracking of oil and gas pipelines. *Journal of Natural Gas Science and Engineering 71*, 102971. https://doi.org/10.1016/j.jngse.2019.102971

ASTM G1 (2017). *Standard Practice for Preparing, Cleaning, and Evaluating Corrosion Test Specimens*, ASTM International, West Conshohocken, PA.

ASTM G31 (2021). *Standard Guide for Laboratory Immersion Corrosion Testing of Metals*. ASTM International, West Conshohocken, PA.

Bezergianni, S., and Dimitriadis, A. (2013). Comparison between different types of renewable diesel. *Renewable and Sustainable Energy Reviews 21*, 110-116. https://doi.org/10.1016/j.rser.2012.12.042

Cabrini, M., Lorenzi, S., Pastore, T., Pellegrini, S., Burattini, M., and Miglio, R. (2017). Study of the corrosion resistance of austenitic stainless steels during conversion of waste to biofuel. *Materials 10*(3), 325. https://doi.org/10.3390/ma10030325

Cavani, F., Albonetti, S., Basile, F., and Gandini, A. (Eds.). (2016). *Chemicals and Fuels from Bio-based Building Blocks*. Wiley-VCH Verlag GmBH & Co. KGaA.

Chozhavendhan, S., Vijay Pradhap Singh, M., Fransila, B., Praveen Kumar, R., and Karthiga Devi, G. (2020). A review on influencing parameters of biodiesel production and purification processes. *Current Research in Green and Sustainable Chemistry, 1-2*, 1-6. https://doi.org/10.1016/j.crgsc.2020.04.002

da Mota, S. A. P., Mancio, A. A., Lhamas, D. E. L., de Abreu, D. H., da Silva, M. S., dos Santos, W. G., de Castro, D. A. R., de Oliveira, R. M., Araújo, M. E., Borges, L. E. P., and Machado, N. T. (2014). Production of green diesel by thermal catalytic cracking of crude palm oil (*Elaeis guineensis* Jacq) in a pilot plant. *Journal of Analytical and Applied Pyrolysis 110*, 1-11. https://doi.org/10.1016/j.jaap.2014.06.011

Douvartzides, S. L., Charisiou, N. D., Papageridis, K. N., and Goula, M. A. (2019). Green diesel: Biomass feedstocks, production technologies, catalytic research, fuel properties and performance in compression ignition internal combustion engines. *Energies 12*(5), 809. https://doi.org/10.3390/en12050809

Farelas, F., Galicia, M., Brown, B., Nesic S., and Castaneda, H. (2010). Evolution of dissolution processes at the interface of carbon steel corroding in a CO_2 environment studied by EIS. *Corrosion Science 52*(2), 509-517, doi: https://doi.org/10.1016/j.corsci.2009.10.007.

Groysman, A. (2017). Corrosion problems and solutions in oil, gas, refining and petrochemical industry. *Koroze a Ochrana Materialu 61*(3), 100-117. https://doi.org/10.1515/kom-2017-0013

Kant Bhatia, S., Kant Bhatia, R., Jeon, J.-M., Pugazhendhi, A., Kumar Awasthi, M., Kumar, D., Kumar, G., Yoon, J.-J., and Yang, Y.-H. (2021). An overview on advancements in biobased transesterification methods for biodiesel production: Oil resources, extraction, biocatalysts, and process intensification technologies. *Fuel 285*, 119117. https://doi.org/10.1016/j.fuel.2020.119117

Keiser, J. R., Howell, M., Lewis, S. A., and Connatser, R. M. (2012). Corrosion studies of raw and treated biomass-derived pyrolysis oils. *Corrosion 2012*. https://www.onepetro.org/conference-paper/NACE-2012-1645

Mailaram, S., Kumar, P., Kunamalla, A., Saklecha, P., and Maity, S. K. (2021). Biomass, biorefinery, and biofuels. *Sustainable Fuel Technologies Handbook* (pp. 51-87). Elsevier. https://doi.org/10.1016/B978-0-12-822989-7.00003-2

Mansoori, H., Mirzaee, R., Esmaeilzadeh, F., Vojood, A., and Dowrani, A. S. (2017). Pitting corrosion failure analysis of a wet gas pipeline. *Engineering Failure Analysis 82*, 16-25. https://doi.org/10.1016/j.engfailanal.2017.08.012

Marroquín, G., Ancheyta, J., and Díaz, J. A. I. (2004). On the effect of reaction conditions on liquid phase sulfiding of a NiMo HDS catalyst. *Catalysis Today 98*(1-2), 75-81. https://doi.org/10.1016/j.cattod.2004.07.021

Marroquín-Sánchez, G., and Ancheyta-Juárez, J. (2001). Catalytic hydrotreating of middle distillates blends in a fixed-bed pilot reactor. *Applied Catalysis A: General, 207*(1-2), 407-420. https://doi.org/10.1016/S0926-860X(00)00683-9

NACE RP0775 (2018). *Preparation, Installation, Analysis, and Interpretation of Corrosion Coupons in Oilfield Operations*. NACE International, Houston, Texas

NACE TM0169/ASTM G31 (2021). *Standard Guide for Laboratory Immersion Corrosion Testing of Metals*.

Perego, C., and Ricci, M. (2012). Diesel fuel from biomass. *Catalysis Science & Technology 2*(9), 1776-1786. https://doi.org/10.1039/C2CY20326J

Salazar-Jiménez, J. A. (2015). Introducción al fenómeno de corrosión: Tipos, factores que influyen y control para la protección de materiales (Nota técnica). *Revista Tecnología en Marcha 28*(3), 127. https://doi.org/10.18845/tm.v28i3.2417

Sotelo-Boyas, R., Trejo-Zarraga, F., and Jesus Hernandez-Loyo, F. de. (2012). Hydroconversion of triglycerides into green liquid fuels. I. Karam (Ed.), *Hydrogenation*. InTech. https://doi.org/10.5772/48710

Tabatabaei, M., Aghbashlo, M., Dehhaghi, M., Panahi, H. K. S., Mollahosseini, A., Hosseini, M., and Soufiyan, M. M. (2019). Reactor technologies for biodiesel production and processing: A review. *Progress in Energy and Combustion Science 74*, 239-303. https://doi.org/10.1016/j.pecs.2019.06.001

Verduzco, L. F. R., Anell, J. A. A., Allieri, M. A. A., Ramirez, M. del R. S. L., García, L. D., Rivera, B. L. M., and Rodriguez, J. E. R. (2020). *Hydrodeoxigenation Process of Vegetable Oils for Obtaining Green Diesel* (United States Patent Núm. US10858594B2). https://patents.google.com/patent/US10858594B2/en